A Method Based on Linear Matrix Inequalities to Design a Wide-Area Damping Controller Resilient to Permanent Communication Failures

Murilo E. C. Bento, *Student Member, IEEE*, and Rodrigo A. Ramos, *Senior Member, IEEE*

***Abstract*—One of the main advantages of the wide-area measurement systems in the small-signal stability of the electric power systems is to use synchrophasor data from the phasor measurement units (PMUs) for the operation of a central controller, or wide-area damping controller (WADC), to improve the damping ratio of the low-frequency oscillation modes. However, cyber-attacks in the PMU measurements can lead to permanent communication failure of the WADC channels and, therefore, the dynamic performance of the power system can be damaged. Besides, the signals for this controller are from different locations and thus they present time delays that can also damage the power system dynamic performance. This article introduces a method based on linear matrix inequalities to design a WADC robust to power system operation uncertainties, time-delay uncertainties, and permanent communication failure of the WADC channels. The proposed method was applied and evaluated in the IEEE 68-bus system by modal analysis and time-domain nonlinear simulations.**

***Index Terms*—Linear matrix inequalities (LMI), oscillatory dynamics damping control, power system small-signal stability, uncertainties, wide-area damping controller (WADC).**

I. Introduction

ADVANCES in information technology have enabled the creation of wide-area measurement systems (WAMS) able to acquiring power system electrical measurements through phasor measurement units (PMUs) installed in certain system locations with high sampling rates and synchronism due to the use of global positioning system (GPS) [1]. This measurement system aroused the interest of the scientific community in developing tools for power system monitoring [2], protection [3], and control [4]–[7].

One of the biggest benefits of synchronized data in small-signal stability is the operation of a designed wide-area damping controller (WADC) or central controller for the improvement of the damping ratio of the electromechanical oscillation modes of the power systems. Usually, the oscillation modes are improved by using power system stabilizers (PSSs) providing a control signal to the automatic voltage regulators (AVRs) located near the synchronous generators [8]. The PSSs are effective in improving local oscillation modes in the frequency range 0.8–2.0 Hz [9]–[11]. However, they have limited effect of improving interarea modes in the frequency range 0.2–0.8 Hz.

The WADC can be constructed to be a controller with multiple inputs and outputs and thus, using different combinations of remote and synchronized signals, the improvement of interarea modes can be achieved [12]. Unlike PSS-type damping controllers, the design of WADC-type controllers requires additional challenges. This has motivated the scientific community to do research to give an appropriate central controller for electric power system and such research is still under development.

A. Literature Review

Methods based on linear matrix inequalities (LMIs) [13], [14], linear quadratic regulator [15], genetic algorithms [16], and others have been formulated in the last decade for the WADC design considering different characteristics. The time delays in transmitting PMU measurements through communication channels to the WADC were the first concern of the researchers. A solution was to consider a fixed time delay given by different transfer functions orders of the Padé approximation. Different communication channels can have different time delays but if we consider a buffer that holds data packets from all channels up to a maximum fixed time, this proposal to use a fixed time delay makes sense. The authors in [17] presented a central controller design based on functions such as spectral abscissa, H_∞ norm and complex stability radius using the second-order Padé approximation for the time delays. The authors in [18] used the second-order representation, a gain scheduling technique, and decision tree approach to design an adaptive WADC. The second-order representation was also used by the author in [19] to design a robust WADC using genetic algorithms. A robust linear quadratic Gaussian-based wide-area damping controller is proposed in [20] using the third-order Padé approximation.

The next step of the researches was to consider time-varying delay in the WADC channels. The authors in [21] pointed out that if the channels are made by optical fiber cables, the delay could be of the order 100–150 ms. A network predictive control approach was proposed by the authors in [22] to handle time-varying delays. The authors in [23] used a toolbox called

Manuscript received March 8, 2020; revised July 16, 2020 and October 1, 2020; accepted October 6, 2020. Date of publication October 23, 2020; date of current version August 26, 2021. This work was supported in part by the São Paulo Research Foundation (FAPESP) under Grant 2015/24245-8 and Grant 2018/20104-9, and in part by the Coordenação de Aperfeiçoamento de Pessoal de Nível Superior - Brasil (CAPES) under Grant 001. *(Corresponding author: Murilo E. C. Bento.)*

The authors are with the Sao Carlos School of Engineering, University of Sao Paulo, Sao Carlos 13566-590, Brazil (e-mail: murilo.bento@usp.br; rodrigo.ramos@ieee.org).

Digital Object Identifier 10.1109/JSYST.2020.3029693

SimEvents in the MatLab software to consider the variable time delays. An adaptive delay compensation is used by the authors in [24] for power system with photovoltaic plant. The authors in [25] incorporated a time delay model in the control design stage to find the time-delay margin of the central controller. The authors in [26] and [27] proposed methods based on fuzzy theory to deal with delays and measures.

Central controller operation requires data transmission through communication channels that are susceptible to cyber-attacks and failures. The protocol employed by PMUs to transmit the synchronized data are described in the IEEE C37.118 standards [28]. Nevertheless, this protocol is susceptible to cyber-attacks such as denial-of-service (DoS) attacks, false data injection attacks, and cyber-physical switching attacks and they can damage the power system dynamic performance [29]. In [30], the authors demonstrated that a certain designed DoS attack sequence on the PMU communication channels can make the power system unstable. Recently, the authors in [31] investigated how delayed, disordered, dropped, and distorted data affect the power system operation and the results showed that these contingencies can damage the power system dynamic performance. As per the author's knowledge few works are available in the literature considering this issue. The authors in [32] considered a two-level control structure, PSS (local signals), more WADC (wide-area signals), and when a failure is detected in the WADC channels, the control structure operates only with the local signals. The authors in [33] proposed to use a reconfiguration of the central controller when a communication channel failure occurs, but this failure must be temporary. The authors in [34]–[36] proposed to employ redundant communication signals when a channel failure occurs but this strategy can have a limited effect. The authors in [37] proposed to use the two-state Gilbert-Elliott model to represent the stochastic data-dropout in the communication link. Different from [32]–[37], a new strategy to handle with permanent communication failure of the WADC channels will be presented and evaluated.

B. Contributions

This article presents an algorithm based on LMIs to design a WADC robust to multiple operating conditions, time-delay uncertainties, and to the permanent communication failure of the WADC channels. The PSSs available in the power system will be considered fixed and the purpose will be to find the WADC parameters for a two-level control structure operation described in Fig. 1, where G_n is the nth synchronous generator, $\Delta\omega_n$ is the nth generator speed signal deviation, and V_{T_n} is the nth generator terminal signal. Unlike the works already published, the contributions of this article can be summarized as follows.

1) The proposed algorithm is based on power system linear models and, then, a set of possible power system operating conditions are linearized around the equilibrium conditions and the goal is to improve the damping ratio of the low-frequency oscillation modes of these conditions.
2) The second-order Padé approximation will be employed to formulate the time-delay model regarding a lower and upper time-delay range. The objective is to guarantee the stability of the system within this range of time-delay uncertainties.
3) A strategy to deal with permanent communication failure will be considered in the control design stage. Thus, even with a permanent failure at the input or output of the central controller, there will be a guarantee of stability and dynamic performance of the closed loop system.
4) The proposed algorithm will use a polytopic model and, then, the resulting central controller will provide quadratic stability for the closed loop system.

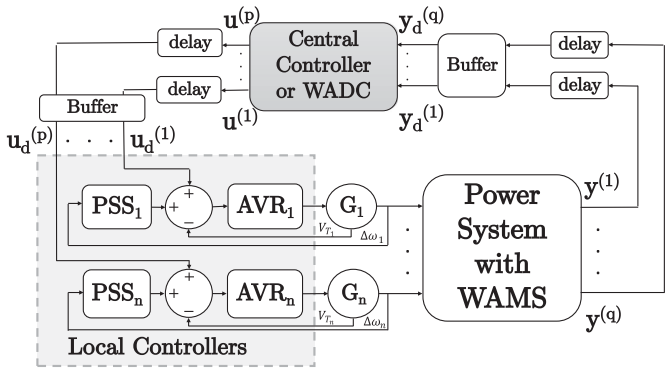

Fig. 1. Power system two-level control structure.

The proposed algorithm was evaluated by modal analysis and time-domain nonlinear simulations in the IEEE 68-bus, 16-machine, 5-area system, the highest benchmark model for small-signal stability studies available in [38].

C. Article Organization

This article presents the following organization. Section II introduces the models of the power system, time delay, central controller, and the strategy for dealing with the permanent communication failure; Section III presents the proposed algorithm based on LMIs to design the central controller; Section IV provides the application of the proposed algorithm in the IEEE 68-bus system; and Section V concludes the article.

II. Modeling

A. Power System Model

In small-signal stability studies, the differential-algebraic nonlinear state-space equations of the power systems can be linearized around each equilibrium condition resulting in the following linear model [39]:

$$\dot{\mathbf{x}}_j = \mathbf{A}_j\mathbf{x}_j + \mathbf{B}_j\mathbf{u}_{\mathbf{d}j} \tag{1}$$

$$\mathbf{y}_j = \mathbf{C}_j\mathbf{x}_j \tag{2}$$

where $\mathbf{x} \in \mathbb{R}^n$ represents the state-space vector, $\mathbf{y} \in \mathbb{R}^p$ represents the output vector (p generator speed signals estimated by PMU data), $\mathbf{u_d} \in \mathbb{R}^p$ represents the input vector (p control signals to the p AVRs), $j = 1, ..., N$ is the number of operating conditions of the system and the matrices of the linear model presents the following dimensions $\mathbf{A} \in \mathbb{R}^{n\times n}$, $\mathbf{B} \in \mathbb{R}^{n\times p}$ and $\mathbf{C} \in \mathbb{R}^{p\times n}$.

B. Time-Delay Model

The pure time delays (e^{-Ts}) at the input and output of the central controller can be represented by a polynomial transfer function through the Padé approximation whose order can be defined by the designer [40]. Recent research such as [15], [17], and [41] used the second-order Padé approximation given by

$$\mathbf{G_d}(s) = \frac{6 - 2Ts}{6 + 4Ts + T^2 s^2} = \frac{-\frac{2}{T}s + \frac{6}{T^2}}{s^2 + \frac{4}{T}s + \frac{6}{T^2}} \tag{3}$$

where T is the time delay in the WADC channels. Further details of this representation in transfer functions can be found in the reference [40]. This transfer function representation can be also represented by state-space equations given by

$$\dot{\mathbf{x}}_\mathbf{d} = \mathbf{A_d}\mathbf{x_d} + \mathbf{B_d}\mathbf{u_d} \tag{4}$$

$$\mathbf{y_d} = \mathbf{C_d}\mathbf{x_d} \tag{5}$$

and the matrices $\mathbf{A_d} \in \mathbb{R}^{2p\times 2p}$, $\mathbf{B_d} \in \mathbb{R}^{2p\times p}$, and $\mathbf{C_d} \in \mathbb{R}^{p\times 2p}$ present the following canonical representation

$$\mathbf{A_d} = \begin{bmatrix} \mathbf{a}_{\mathbf{d}1} \cdots & \mathbf{0} \\ \vdots \quad \ddots & \vdots \\ \mathbf{0} \quad \cdots & \mathbf{a}_{\mathbf{d}p} \end{bmatrix}, \mathbf{B_d} = \begin{bmatrix} \mathbf{b}_{\mathbf{d}1} \cdots & \mathbf{0} \\ \vdots \quad \ddots & \vdots \\ \mathbf{0} \quad \cdots & \mathbf{b}_{\mathbf{d}p} \end{bmatrix} \tag{6}$$

$$\mathbf{C_d} = \begin{bmatrix} \mathbf{c}_{\mathbf{d}1} \cdots & \mathbf{0} \\ \vdots \quad \ddots & \vdots \\ \mathbf{0} \quad \cdots & \mathbf{c}_{\mathbf{d}p} \end{bmatrix} \tag{7}$$

where for $k = 1, ..., p$

$$\mathbf{a}_{\mathbf{d}k} = \begin{bmatrix} 0 & -\frac{6}{T^2} \\ 1 & -\frac{4}{T} \end{bmatrix}, \mathbf{b}_{\mathbf{d}k} = \begin{bmatrix} \frac{6}{T^2} \\ -\frac{2}{T} \end{bmatrix}, \mathbf{c}_{\mathbf{d}k} = \begin{bmatrix} 0 & 1 \end{bmatrix} \tag{8}$$

and, then, $\mathbf{G_d}(s) = \mathbf{C_d}(s\mathbf{I} - \mathbf{A_d})^{-1}\mathbf{B_d}$.

Each channel of the control structure can have different time delays. However, if we consider a buffer in the input and output of the WADC, signals from all channels can be held within a certain limit $[T_{\min}, T_{\max}]$. If the time delay exceeds this limit, the signal will be considered lost. So the goal is to find the time delay limits on the input and output of the central controller.

We can use the state-space model (4) and (5) to represent the time delay in the input $(\mathbf{i})$ and output $(\mathbf{o})$ of the central controller results in the following state-space equations:

$$\dot{\mathbf{x}}_\mathbf{di} = \mathbf{A_{di}}\mathbf{x_{di}} + \mathbf{B_{di}}\mathbf{u} \tag{9}$$

$$\mathbf{u_d} = \mathbf{C_{di}}\mathbf{x_{di}} \tag{10}$$

$$\dot{\mathbf{x}}_\mathbf{do} = \mathbf{A_{do}}\mathbf{x_{do}} + \mathbf{B_{do}}\mathbf{y} \tag{11}$$

$$\mathbf{y_{do}} = \mathbf{C_{do}}\mathbf{x_{do}} \tag{12}$$

where $\mathbf{x_{di}}$ and $\mathbf{x_{do}}$ are the state vectors related to the input and output time-delay models, respectively, $\mathbf{u} = [\, u^{(1)} \cdots u^{(p)} \,]^T \in \mathbb{R}^p$ is the vector with p the control signals provided by the WADC, and $\mathbf{y_d} = [\, y_d^{(1)} \cdots y_d^{(p)} \,]^T \in \mathbb{R}^p$ is the vector with p the speed signals for the WADC.

The state-space equations of the power system (1) and (2), input time-delay model (9) and (10), and output time-delay model (11) and (12) can be joined and the result is the following state-space equations:

$$\dot{\bar{\mathbf{x}}}_j = \bar{\mathbf{A}}_j\bar{\mathbf{x}}_j + \bar{\mathbf{B}}\mathbf{u}_j \tag{13}$$

$$\mathbf{y_{d}}_j = \bar{\mathbf{C}}\bar{\mathbf{x}}_j \tag{14}$$

where $\mathbf{x}_j = [\, \mathbf{x}_j^T \ \mathbf{x_{di}}^T \ \mathbf{x_{do}}^T \,]^T$, $j = 1, ..., N$ and

$$\bar{\mathbf{A}}_j = \begin{bmatrix} \mathbf{A}_j & \mathbf{B}_j\mathbf{C_{di}} & \mathbf{0} \\ \mathbf{0} & \mathbf{A_{di}} & \mathbf{0} \\ \mathbf{B_{do}}\mathbf{C}_j & \mathbf{0} & \mathbf{A_{do}} \end{bmatrix}, \bar{\mathbf{B}} = \begin{bmatrix} \mathbf{0} \\ \mathbf{B_{di}} \\ \mathbf{0} \end{bmatrix} \tag{15}$$

$$\bar{\mathbf{C}} = \begin{bmatrix} \mathbf{0}\ \mathbf{0}\ \mathbf{C_{do}} \end{bmatrix} \tag{16}$$

and $\bar{\mathbf{A}}_j \in \mathbb{R}^{r\times r}$, $\bar{\mathbf{B}} \in \mathbb{R}^{r\times p}$ and $\bar{\mathbf{C}} \in \mathbb{R}^{p\times r}$.

C. WADC or Central Controller

The main goal of this article is to design a central controller that can be represented as a transfer function matrix as follows:

$$\mathbf{WADC}(s) = \begin{bmatrix} cc_{11}(s) \cdots & cc_{1p}(s) \\ \vdots \quad \ddots & \vdots \\ cc_{p1}(s) \cdots & cc_{pp}(s) \end{bmatrix} \tag{17}$$

where each transfer function $cc_{kl}(s)$ $(k, l = 1, ..., p)$ will be

$$cc_{kl}(s) = \frac{n_{kl}^2 s^2 + n_{kl}^1 s + n_{kl}^0}{s^2 + a_1 s + a_0} = \frac{b_{kl}^1 s + b_{kl}^0}{s^2 + d_1 s + d_0} + d_{kl}. \tag{18}$$

The state-space equations for the transfer function matrix (17) can be described as

$$\dot{\mathbf{x}}_c = \mathbf{A_c}\mathbf{x_c} + \mathbf{B_c}\mathbf{y_d} \tag{19}$$

$$\mathbf{u} = \mathbf{C_c}\mathbf{x_c} + \mathbf{D_c}\mathbf{y_d} \tag{20}$$

and then $\mathbf{WADC}(c) = \mathbf{C_c}(s\mathbf{I} - \mathbf{A_c})^{-1}\mathbf{B_c} + \mathbf{D_c}$.

A canonical representation will be used in this article for the matrices $\mathbf{A_c} \in \mathbb{R}^{2p\times 2p}$, $\mathbf{B_c} \in \mathbb{R}^{2p\times p}$, $\mathbf{C_c} \in \mathbb{R}^{p\times 2p}$, and $\mathbf{D_c} \in \mathbb{R}^{p\times p}$ and they are described as follows:

$$\mathbf{A_c} = \begin{bmatrix} \mathbf{a}_{\mathbf{c}1} \cdots & \mathbf{0} \\ \vdots \quad \ddots & \vdots \\ \mathbf{0} \quad \cdots & \mathbf{a}_{\mathbf{c}p} \end{bmatrix}, \mathbf{B_c} = \begin{bmatrix} \mathbf{b}_{\mathbf{c}11} \cdots & \mathbf{b}_{\mathbf{c}1p} \\ \vdots \quad \ddots & \vdots \\ \mathbf{b}_{\mathbf{c}p1} \cdots & \mathbf{b}_{\mathbf{c}pp} \end{bmatrix} \tag{21}$$

$$\mathbf{C_c} = \begin{bmatrix} \mathbf{c}_{\mathbf{c}1} \cdots & \mathbf{0} \\ \vdots \quad \ddots & \vdots \\ \mathbf{0} \quad \cdots & \mathbf{c}_{\mathbf{c}p} \end{bmatrix}, \mathbf{D_c} = \begin{bmatrix} d_{11} \cdots & d_{1p} \\ \vdots \quad \ddots & \vdots \\ d_{1p} \cdots & d_{pp} \end{bmatrix} \tag{22}$$

where for $k = 1, ..., p$ and $l = 1, ..., p$

$$\mathbf{a}_{\mathbf{c}k} = \begin{bmatrix} 0 & -a_0 \\ 1 & -a_1 \end{bmatrix}, \mathbf{b}_{\mathbf{c}kl} = \begin{bmatrix} b_{kl}^0 \\ b_{kl}^1 \end{bmatrix} \tag{23}$$

$$\mathbf{c}_{\mathbf{c}k} = \begin{bmatrix} 0 & 1 \end{bmatrix}. \tag{24}$$

D. Closed Loop System

The state-space equations of the closed loop system is the combination of power system model with time-delay model (13) and (14) and the central controller equations (19) and (20) and it can be given as

$$\dot{\widehat{\mathbf{x}}}_j = \widehat{\mathbf{A}}_j\widehat{\mathbf{x}}_j \tag{25}$$

where the closed loop state vector is $\widehat{\mathbf{x}}_j = [\,\bar{\mathbf{x}}^T\ \mathbf{x}_\mathbf{c}^T\,]^T$, $j = 1, ..., N$ and the matrix $\widehat{\mathbf{A}}_j \in \mathbb{R}^{m\times m}$ is

$$\widehat{\mathbf{A}}_j = \begin{bmatrix} \bar{\mathbf{A}}_j + \bar{\mathbf{B}}\mathbf{D}_\mathbf{c}\bar{\mathbf{C}} & \bar{\mathbf{B}}\mathbf{C}_\mathbf{c} \\ \mathbf{B}_\mathbf{c}\bar{\mathbf{C}} & \mathbf{A}_\mathbf{c} \end{bmatrix}. \tag{26}$$

We can also define the closed loop system using the following representations:

$$\mathbf{A}_{\mathbf{a}j} = \begin{bmatrix} \bar{\mathbf{A}}_j & \bar{\mathbf{B}}\mathbf{C}_\mathbf{c} \\ \mathbf{0} & \mathbf{A}_\mathbf{c} \end{bmatrix}, \mathbf{B}_\mathbf{a} = \begin{bmatrix} \bar{\mathbf{B}} & \mathbf{0} \\ \mathbf{0} & \mathbf{I} \end{bmatrix} \tag{27}$$

$$\mathbf{C}_\mathbf{a} = \begin{bmatrix} \bar{\mathbf{C}} & \mathbf{0} \end{bmatrix}, \mathbf{G}_\mathbf{a} = \begin{bmatrix} \mathbf{D}_\mathbf{c} & \mathbf{B}_\mathbf{c} \end{bmatrix}^T \tag{28}$$

where $\mathbf{G}_\mathbf{a} \in \mathbb{R}^{3p\times p}$ and then

$$\widehat{\mathbf{A}}_j = \mathbf{A}_{\mathbf{a}j} + \mathbf{B}_\mathbf{a}\mathbf{G}_\mathbf{a}\mathbf{C}_\mathbf{a}. \tag{29}$$

If the matrices of the power system operation conditions and the poles of the central controller are known, the matrices $\mathbf{A}_{\mathbf{a}j}$, $\mathbf{B}_\mathbf{a}$, and $\mathbf{C}_\mathbf{a}$ are fixed and the control problem is to find the matrix $\mathbf{G}_\mathbf{a}$ or the matrices $\mathbf{B}_\mathbf{c}$ and $\mathbf{D}_\mathbf{c}$. It is a common practice in small-signal stability studies to design the controller to ensure a minimum damping (ζ_0) for all eigenvalues of the closed loop system. In this article, it was decided to guarantee a minimum damping ratio of 5% because the authors in [42] considered satisfactory for the power system dynamic performance.

E. Robustness to Permanent Communication Failure

When a permanent communication failure of the WADC channels occurs, the synchronized data related to this channel will be lost and this situation can be interpreted as zeroing columns or rows of the matrices $\mathbf{B}_j$ and $\mathbf{C}_j$ associated to the lost channel. In this article, only one permanent communication failure at a time will be considered. The input or the output of the central controller.

When the central controller is operating with p inputs (generator speed signals) and p outputs (WADC control signals) and the input s ($s \in \mathbb{N}, 1 \le s \le p$) is lost, the sth row of the matrix $\mathbf{C}_j$ must be zeroed and this new matrix will be $\mathbf{C}_j^s$. When the output t ($t \in \mathbb{N}, 1 \le t \le p$) is lost, the tth column of the matrix $\mathbf{B}_j$ must be zeroed and this new matrix will be $\mathbf{B}_j^t$. The modifications in the matrices $\mathbf{B}_j$ and $\mathbf{C}_j$ will modify the matrix $\bar{\mathbf{A}}_j$ in (15) and, consequently, the matrix $\mathbf{A}_{\mathbf{a}j}$ in (27). The matrices $\bar{\mathbf{B}}$ (15) and $\bar{\mathbf{C}}$ (16) will be the same as the matrices $\mathbf{B}_\mathbf{a}$ (27) and $\mathbf{C}_\mathbf{a}$ (28). Then, we can establish three sets of closed loop systems: 1) The central controller working with all channels [see (29)], 2) one permanent communication loss of the WADC input signal [see (30)], and 3) one permanent communication loss of the WADC output signal [see (31)]

$$\widetilde{\mathbf{A}}_q = \mathbf{A}_{\mathbf{a}j}^s + \mathbf{B}_\mathbf{a}\mathbf{G}_\mathbf{a}\mathbf{C}_\mathbf{a} \tag{30}$$

$$\breve{\mathbf{A}}_q = \mathbf{A}_{\mathbf{a}j}^t + \mathbf{B}_\mathbf{a}\mathbf{G}_\mathbf{a}\mathbf{C}_\mathbf{a} \tag{31}$$

for $j = 1, ..., N$, $s = 1, ..., p$, $t = 1, ..., p$, and $q = 1, ..., N \cdot p$.

Based on this formulation, the guarantee of robustness to permanent communication failure of the WADC channels is to find a central controller that provides a satisfactory damping ratio for the closed loop systems (30) and (31) considering all combinations of one channel loss.

III. Proposed Algorithm Based on LMIs

The proposed algorithm is based on Lyapunov stability theory. The main idea is to find the matrices $\mathbf{A}_\mathbf{c}$, $\mathbf{B}_\mathbf{c}$, and $\mathbf{D}_\mathbf{c}$ of the central controller and a matrix $\mathbf{P}$ that can prove local stability for each operation condition [43]. Based on Lyapunov stability theory, each equilibrium of (25) is locally stable if and only if there exist matrices $\mathbf{A}_\mathbf{c}$, $\mathbf{B}_\mathbf{c}$, $\mathbf{D}_\mathbf{c}$, and $\mathbf{P}$, such that

$$\mathbf{P}^T = \mathbf{P} \succ \mathbf{0} \tag{32}$$

$$\widehat{\mathbf{A}}_j^T\mathbf{P} + \mathbf{P}\widehat{\mathbf{A}}_j \prec \mathbf{0} \tag{33}$$

$$\widetilde{\mathbf{A}}_q^T\mathbf{P} + \mathbf{P}\widetilde{\mathbf{A}}_q \prec \mathbf{0} \tag{34}$$

$$\breve{\mathbf{A}}_q^T\mathbf{P} + \mathbf{P}\breve{\mathbf{A}}_q \prec \mathbf{0} \tag{35}$$

for $j = 1, ..., N$ and the notations $\mathbf{V} \succ \mathbf{0}$ and $\mathbf{W} \prec \mathbf{0}$ indicate positive and negative definiteness of matrices $\mathbf{V}$ and $\mathbf{W}$, respectively [43].

As mentioned in Section II-D, local stabilization is not enough to ensure an adequate performance for the closed loop power system. To fulfill the minimum damping ratio criterion (ζ_0), we must find the matrices $\mathbf{A}_\mathbf{c}$, $\mathbf{B}_\mathbf{c}$, $\mathbf{D}_\mathbf{c}$, and $\mathbf{P}$, such that

$$\mathbf{P}^T = \mathbf{P} \succ \mathbf{0} \tag{36}$$

$$\begin{bmatrix} \sin(\theta)\left(\widehat{\mathbf{A}}_j^T\mathbf{P} + \mathbf{P}\widehat{\mathbf{A}}_j\right) & \cos(\theta)\left(\widehat{\mathbf{A}}_j^T\mathbf{P} - \mathbf{P}\widehat{\mathbf{A}}_j\right) \\ \cos(\theta)\left(\widehat{\mathbf{A}}_j^T\mathbf{P} - \mathbf{P}\widehat{\mathbf{A}}_j\right)^T & \sin(\theta)\left(\widehat{\mathbf{A}}_j^T\mathbf{P} + \mathbf{P}\widehat{\mathbf{A}}_j\right) \end{bmatrix} \prec \mathbf{0} \tag{37}$$

$$\begin{bmatrix} \sin(\theta)\left(\widetilde{\mathbf{A}}_q^T\mathbf{P} + \mathbf{P}\widetilde{\mathbf{A}}_q\right) & \cos(\theta)\left(\widetilde{\mathbf{A}}_q^T\mathbf{P} - \mathbf{P}\widetilde{\mathbf{A}}_q\right) \\ \cos(\theta)\left(\widetilde{\mathbf{A}}_q^T\mathbf{P} - \mathbf{P}\widetilde{\mathbf{A}}_q\right)^T & \sin(\theta)\left(\widetilde{\mathbf{A}}_q^T\mathbf{P} + \mathbf{P}\widetilde{\mathbf{A}}_q\right) \end{bmatrix} \prec \mathbf{0} \tag{38}$$

$$\begin{bmatrix} \sin(\theta)\left(\breve{\mathbf{A}}_q^T\mathbf{P} + \mathbf{P}\breve{\mathbf{A}}_q\right) & \cos(\theta)\left(\breve{\mathbf{A}}_q^T\mathbf{P} - \mathbf{P}\breve{\mathbf{A}}_q\right) \\ \cos(\theta)\left(\breve{\mathbf{A}}_q^T\mathbf{P} - \mathbf{P}\breve{\mathbf{A}}_q\right)^T & \sin(\theta)\left(\breve{\mathbf{A}}_q^T\mathbf{P} + \mathbf{P}\breve{\mathbf{A}}_q\right) \end{bmatrix} \prec \mathbf{0} \tag{39}$$

where $j = 1, ..., N$ and $\theta = \arccos(\zeta_0)$.

The matrix inequalities (37)–(39) are bilinear (BMI) because there is a multiplication between the variables $\mathbf{P}$ and $\mathbf{A}_\mathbf{c}$, $\mathbf{B}_\mathbf{c}$, and $\mathbf{D}_\mathbf{c}$. Section III-A will present a strategy to deal with BMIs transforming into a linear problem.

A. Strategy to Deal With the BMIs

We can expand the elements of (37)–(39) as

$$\mathbf{P}\widehat{\mathbf{A}}_j = \mathbf{P}\mathbf{A}_{\mathbf{a}j} + \mathbf{P}\mathbf{B}_\mathbf{a}\mathbf{G}_\mathbf{a}\mathbf{C}_\mathbf{a} \tag{40}$$

$$\mathbf{P}\widetilde{\mathbf{A}}_q = \mathbf{P}\mathbf{A}_{\mathbf{a}j}^s + \mathbf{P}\mathbf{B}_\mathbf{a}\mathbf{G}_\mathbf{a}\mathbf{C}_\mathbf{a} \tag{41}$$

$$\mathbf{P}\breve{\mathbf{A}}_q = \mathbf{P}\mathbf{A}_{\mathbf{a}j}^t + \mathbf{P}\mathbf{B}_\mathbf{a}\mathbf{G}_\mathbf{a}\mathbf{C}_\mathbf{a} \tag{42}$$

and the multiplication $\mathbf{PB_aG_a}$ makes the problem bilinear. If we define

$$\mathbf{N} \cdot \mathbf{M} = \mathbf{PB_aG_a} \tag{43}$$

where the matrix $\mathbf{N}$ will be a variable of the problem and the matrix $\mathbf{M}$ will be known, the problem becomes linear.

The dimension of $\mathbf{N} \cdot \mathbf{M}$ must be $\mathbb{R}^{3p \times p}$ and, then, the designer can define a parameter h that defines the following matrix dimensions $\mathbf{N} \in \mathbb{R}^{3p \times h}$ and $\mathbf{M} \in \mathbb{R}^{h \times p}$. It is possible to see that the choice of the parameter h will affect the number of variables in $\mathbf{N}$ and this can affect the LMI-based algorithm convergence. In this article, it was defined $h = p$. This choice proved to be effective in the design of wide-area damping controllers. However, if there are convergence problems, the value of this parameter h can be changed. In addition, to use this strategy, the matrices $\mathbf{A_a}$, $\mathbf{B_a}$, and $\mathbf{C_a}$ must be reduced to following dimensions $3p \times 3p$, $3p \times 3p$ and $p \times 3p$ and the variable matrix P must have the dimension $3p \times 3p$.

As already said, the matrix $\mathbf{M}$ will be known and each element of the matrix will be randomly generated in a range $[L_{\min}, L_{\max}]$. In this article, the limits were defined as $L_{\min} = 0$ and $L_{\max} = 1$.

After the convergence of the LMIs, the matrix $\mathbf{G_a}$ in (43) can be obtained as

$$\mathbf{G_a} = \left(\mathbf{B_a}^T \cdot \mathbf{B_a}\right)^{-1} \cdot \mathbf{B_a}^T \cdot \mathbf{P}^{-1} \cdot \mathbf{N} \cdot \mathbf{M}. \tag{44}$$

B. Algorithm

The step-by-step algorithm based on LMIs to design the WADC is described as follows.

Step 01: Define the set of operating conditions (N), the number of inputs/outputs of the WADC (p), and obtain the linear models for each condition $(\mathbf{A}_j, \mathbf{B}_j, \mathbf{C}_j, j = 1, ..., N)$.

Step 02: Set the minimum $(T_{\min})$ and maximum $(T_{\max})$ time-delay values and build the linear models $(\bar{\mathbf{A}}_j, \bar{\mathbf{B}}, \bar{\mathbf{C}}, j = 1, ..., N)$.

Step 03: Choose the poles of the central controller $(\mathbf{A_c})$, build the matrices $\mathbf{A_a}_j$, $\mathbf{B_a}$, and $\mathbf{C_a}$ and reduce them to the dimensions $3p \times 3p$, $3p \times 3p$ and $p \times 3p$, respectively.

Step 04: Generate a random matrix $\mathbf{M}$.

Step 05: Build the following linear matrix inequalities:

$$\mathbf{P} = \mathbf{P}^T \succ \mathbf{0} \tag{45}$$

$$\begin{bmatrix} \sin(\theta)\left(\mathbf{Q}_j^T + \mathbf{Q}_j\right) & \cos(\theta)\left(\mathbf{Q}_j^T - \mathbf{Q}_j\right) \\ \cos(\theta)\left(\mathbf{Q}_j^T - \mathbf{Q}_j\right)^T & \sin(\theta)\left(\mathbf{Q}_j^T + \mathbf{Q}_j\right) \end{bmatrix} \prec \mathbf{0} \tag{46}$$

$$\begin{bmatrix} \sin(\theta)\left(\widetilde{\mathbf{Q}}_q^T + \widetilde{\mathbf{Q}}_q\right) & \cos(\theta)\left(\widetilde{\mathbf{Q}}_q^T - \widetilde{\mathbf{Q}}_q\right) \\ \cos(\theta)\left(\widetilde{\mathbf{Q}}_q^T - \widetilde{\mathbf{Q}}_q\right)^T & \sin(\theta)\left(\widetilde{\mathbf{Q}}_q^T + \widetilde{\mathbf{Q}}_q\right) \end{bmatrix} \prec \mathbf{0} \tag{47}$$

$$\begin{bmatrix} \sin(\theta)\left(\breve{\mathbf{Q}}_q^T + \breve{\mathbf{Q}}_q\right) & \cos(\theta)\left(\breve{\mathbf{Q}}_q^T - \breve{\mathbf{Q}}_q\right) \\ \cos(\theta)\left(\breve{\mathbf{Q}}_q^T - \breve{\mathbf{Q}}_q\right)^T & \sin(\theta)\left(\breve{\mathbf{Q}}_q^T + \breve{\mathbf{Q}}_q\right) \end{bmatrix} \prec \mathbf{0} \tag{48}$$

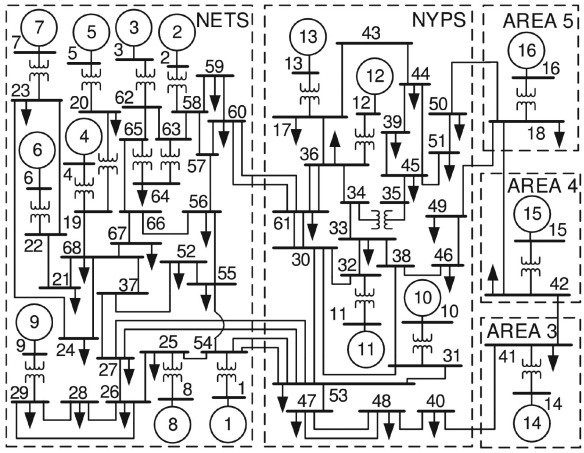

Fig. 2. IEEE 68-bus, 16-machine, 5-area system [38].

where $j = 1, .., N$, $q = 1, ..., N \cdot p$, $\theta = \arccos(\zeta_0)$ and

$$\mathbf{Q}_j = \mathbf{PA_a}_j + \mathbf{NMC_a} \tag{49}$$

$$\widetilde{\mathbf{Q}}_q = \mathbf{PA}_{\mathbf{a}j}^s + \mathbf{NMC_a} \tag{50}$$

$$\breve{\mathbf{Q}}_q = \mathbf{PA}_{\mathbf{a}j}^t + \mathbf{NMC_a} \tag{51}$$

where $s = 1, .., p$ and $t = 1, ..., p$ and the variables are the matrices $\mathbf{P}$ and $\mathbf{N}$.

Step 06: Solve the LMIs (45)–(48) using a solver

Step 07: If a solution is found, go to Step 08; otherwise, go to Step 04.

Step 08: Find the values of the matrices $\mathbf{B_c}$ and $\mathbf{D_c}$ by

$$\begin{bmatrix} \mathbf{D_c} \\ \mathbf{B_c} \end{bmatrix} = \mathbf{G_a} = \left(\mathbf{B_a}^T \cdot \mathbf{B_a}\right)^{-1} \cdot \mathbf{B_a}^T \cdot \mathbf{P}^{-1} \cdot \mathbf{N} \cdot \mathbf{M}. \tag{52}$$

Step 09: The resulting WADC will be

$$\mathbf{WADC}(c) = \mathbf{C_c}\left(s\mathbf{I} - \mathbf{A_c}\right)^{-1}\mathbf{B_c} + \mathbf{D_c}. \tag{53}$$

In this article, the SeDuMi solver was used to solve the LMIs [44].

IV. Test Results and Discussion

The proposed algorithm based on LMIs described in Section III was applied in the IEEE 68-bus, 16-machine, 5-area system described in Fig. 2. This is the highest power system model available in [38] for small-signal stability studies and only one operating condition (BC: Base case) is available. The power system model presents 16 synchronous generators but only generators 1 to 12 have an AVR and a PSS.

A set of power system operation conditions was obtained by increasing the load levels of the areas 1 and 2 to a maximum of 3% and areas 3, 4, and 5 to a maximum of 6%. The operating condition of these maximum load levels will be called C1 case. Table I shows the dominant eigenvalues for the BC and C1 operation conditions. It is possible to see that these modes are interarea oscillation modes in the frequency range 0.2–0.8 Hz. Applying the mode shape analysis, mode M3 of Table I is associated to generator 16 against generators 14 and 15. Modes M2 and M5 are

TABLE I
DOMINANT OSCILLATION MODES OF THE IEEE 68 BUS

Case	Mode	Eigenvalue	Freq. [Hz]	Damping [%]
BC	M1	$-0.1657 \pm 4.8917i$	0.7785	3.3851
	M2	$-0.1184 \pm 3.2665i$	0.5199	3.6236
C1	M3	$+0.0017$	0	-100
	M4	$-0.0755 \pm 3.1521i$	0.5017	2.3933
	M5	$-0.1633 \pm 4.8796i$	0.7766	3.3450

TABLE II
CONTROLLABILITY FACTORS OF M3, M4, AND M5 OF TEST SYSTEM

Generator	Controllability Factors			Available?
	M3	M4	M5	
1	0.0075	0.0924	0.2077	Yes
2	0.0114	0.0484	0.1873	Yes
3	0.0126	0.0736	0.2606	Yes
4	0.0194	0.1340	0.2734	Yes
5	**0.0216**	**0.1218**	**0.2470**	**Yes**
6	0.0211	0.1090	0.2353	Yes
7	0.0134	0.1269	0.2666	Yes
8	0.0088	0.0611	0.1304	Yes
9	**0.0215**	**0.2769**	**0.9234**	**Yes**
10	**0.0349**	**0.1456**	**0.4125**	**Yes**
11	**0.0415**	**0.7405**	**0.8348**	**Yes**
12	**0.0345**	**0.6387**	**0.2949**	**Yes**
13	0.0775	0.1628	0.0330	No
14	0.2158	0.9877	1.0000	No
15	0.3090	0.1636	0.9192	No
16	1.0000	1.0000	0.5272	No

TABLE III
OBSERVABILITY FACTORS OF M3, M4, AND M5 OF THE TEST SYSTEM

Generator	Observability Factors			Measurable?
	M3	M4	M5	
1	1.0000	0.1752	0.0464	Yes
2	1.0000	0.2207	0.0322	Yes
3	1.0000	0.2267	0.0335	Yes
4	1.0000	0.2414	0.0427	Yes
5	1.0000	0.2550	0.0485	Yes
6	1.0000	0.2514	0.0511	Yes
7	1.0000	0.2452	0.0486	Yes
8	1.0000	0.1901	0.0346	Yes
9	1.0000	0.2194	0.0670	Yes
10	1.0000	0.1565	0.0725	Yes
11	1.0000	0.1884	0.0337	Yes
12	**1.0000**	**0.2782**	**0.0411**	**Yes**
13	**1.0000**	**0.4042**	**0.1219**	**Yes**
14	**1.0000**	**1.0000**	**0.6405**	**Yes**
15	**1.0000**	**0.2828**	**1.0000**	**Yes**
16	**1.0000**	**0.8258**	**0.2770**	**Yes**

associated to generator 15 against generators 10–13 and modes M1 and M4 are associated to generator 14 against generators 15 and 16. Then, these modes with low-damping are related to generators that do not have an AVR and a PSS. Nevertheless, the speed signals of generators 13–16 can be estimated and used for the wide-area damping control operation. Therefore, the purpose will be to design a WADC to improve the damping ratio of these operation conditions considering time-delay uncertainties in a specific range and resiliency to permanent communication failure of one WADC channel.

A. Central Controller Design Stage

Before applying the proposed algorithm, we must define the appropriated signals for the input and output of the WADC to be designed. Using the theory of geometric measures [39], Tables II and III present the controllability and observability factors, respectively, for the modes M3, M4, and M5 for the C1 case. Based on the results, it was decided to use 5 signals ($p = 5$) for input and output of the central controller. The generator control signals (WADC output signals) were 5, 9, 10, 11, and 12 and the generator speed signals (WADC input signals) were 12, 13, 14, 15, and 16.

The authors in [21] pointed out that if the channels are made by optical fiber cables, the delay could be of the order 100–150 ms and then, the lower and upper time delays were defined as $T_{\min} = 0.100$ and $T_{\max} = 0.150$, respectively. The poles of the PSSs for this power system are equal to -25 [38] and it was decided to use these poles for the central controller. The matrix $\mathbf{M} \in \mathbb{R}^{p\times p}$ will generate randomly in the range $[L_{\min} = 0, L_{\max} = 1]$. The minimum damping ratio for the closed loop systems will be 5% ($\zeta_0 = 0.05$). The variables will be the matrices $\mathbf{P} \in \mathbb{R}^{m\times m}$ and $\mathbf{N} \in \mathbb{R}^{m\times p}$.

The proposed algorithm based on LMIs was implemented on a machine with Intel Xeon CPU 2.40 GHz, 64-GB RAM running on a Microsoft 10 Home 64-bit, and it took almost 29 min to converge. The resulting central controller WADC-p(s) is presented in (54), shown at the bottom of this page. In order to evaluate the performance of the central controller designed by the approach proposed in this research, three different existing approaches in the literature for central controller designs have been implemented resulting in the WADC-I [15], WADC-II [3], and WADC-III [34] controllers. Approach [15] considers a single point of operation and a fixed time delay given by the second-order Padé approximation. Approach [3] considers a discrete set of operating points, variable communication time delays, but it does not consider communication channel failure. Approach [34] considers a set of operation conditions, fixed time delay given by the second-order Padé approximation, and

$$\text{WADC-p}(s) = \begin{bmatrix} \frac{-0.79s^2-108s-3709}{s^2+50s+625} & \frac{464s^2+3280s+5794}{s^2+50s+625} & \frac{-184s^2-5775s-8002}{s^2+50s+625} & \frac{-4.98s^2-681s-893}{s^2+50s+625} & \frac{-8877s^2-20607s-11847}{s^2+50s+625} \\ \frac{-218s^2-515.5s-304}{s^2+50s+625} & \frac{-340s^2-2397s-3335}{s^2+50s+625} & \frac{2357s^2+7519s+5265}{s^2+50s+625} & \frac{916s^2+12111s+11996}{s^2+50s+625} & \frac{-4.5s^2-1888s-2756}{s^2+50s+625} \\ \frac{1751s^2+9235s+9836}{s^2+50s+625} & \frac{2897s^2+9658s+7503}{s^2+50s+625} & \frac{1487s^2+3144s+1661}{s^2+50s+625} & \frac{120s^2+4011s+12142}{s^2+50s+625} & \frac{8383s^2+17491s+9119}{s^2+50s+625} \\ \frac{2444s^2+5324s+2887}{s^2+50s+625} & \frac{-27s^2-1221s-10880}{s^2+50s+625} & \frac{-249s^2-2971s-2735}{s^2+50s+625} & \frac{11s^2+9301s+9446}{s^2+50s+625} & \frac{4824s^2+13617s+8860}{s^2+50s+625} \\ \frac{-133s^2-6797s-7142}{s^2+50s+625} & \frac{829s^2+2524.5s+1922}{s^2+50s+625} & \frac{74s^2+11741s+12306}{s^2+50s+625} & \frac{395s^2+5415.7s+5832}{s^2+50s+625} & \frac{-177s^2-1562.5s-1955}{s^2+50s+625} \end{bmatrix} \quad (54)$$

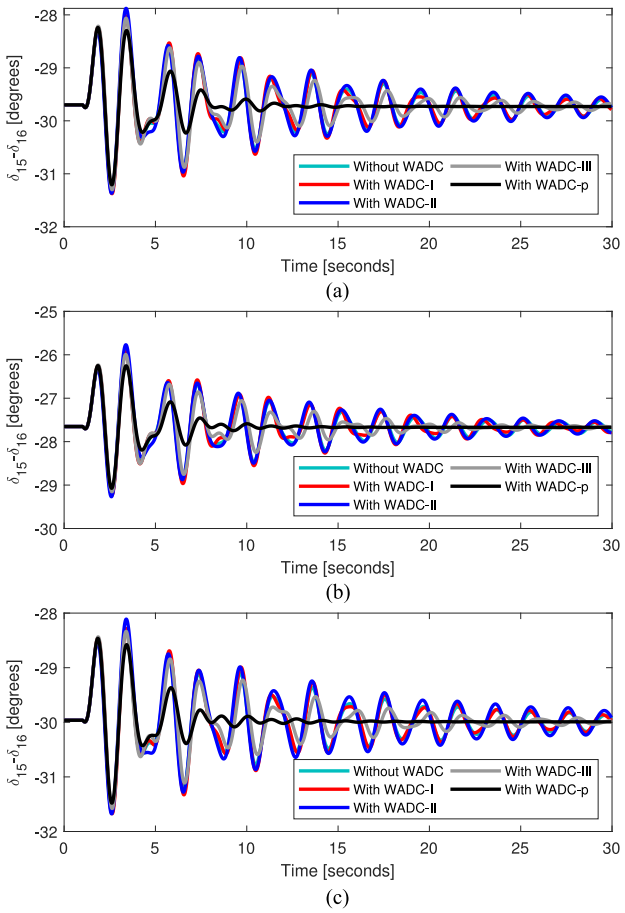

Fig. 3. Angular deviation responses of generators 15 and 16 without the WADC and with WADC-I, WADC-II, WADC-III, and WADC-p for the scenario S1 and (a) C1 operating condition, (b) C2 operating condition, and (c) C3 operating condition.

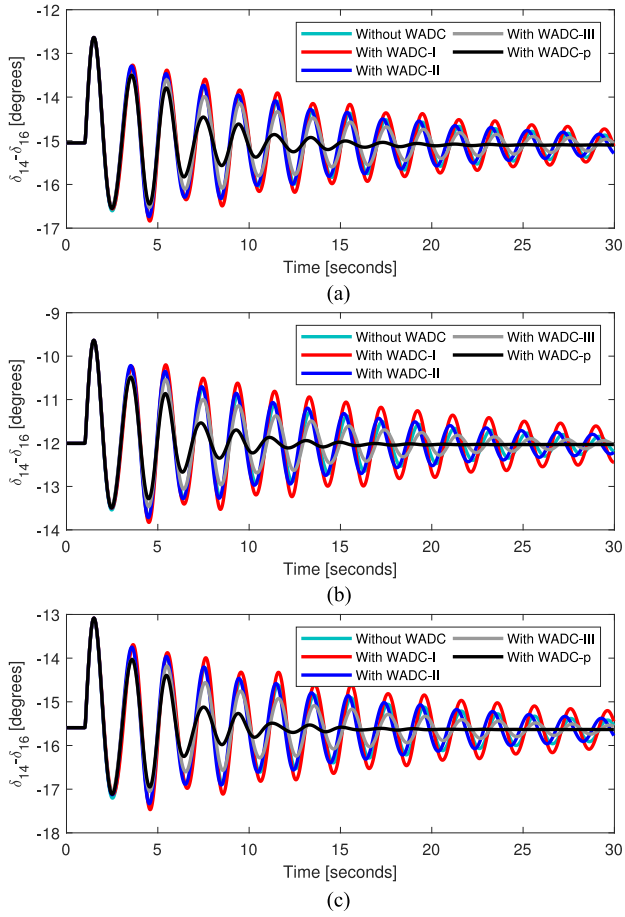

Fig. 4. Angular deviation responses of generators 14 and 16 without the WADC and with WADC-I, WADC-II, WADC-III, and WADC-p for the scenario S2 and (a) C1 operating condition, (b) C2 operating condition, and (c) C3 operating condition.

it provides resiliency against failures using redundant communication signals but this failure must be temporary and the use of redundant signals has limited effect.

B. Time-Domain Nonlinear Simulations

The resulting WADC-p(s) obtained by the proposed algorithm and the WADC-I, WADC-II, and WADC-III obtained by existing methods were evaluated by time-domain nonlinear simulations in the ANATEM software [45]. The central controller will present the same output limits of the PSSs described in [38]. The following operating conditions were evaluated: C1 case already described in the second paragraph of Section IV; C2 case that presents the following load level: increase of 2% in area 1, increase of 3% in area 2, increase of 4% in area 3, increase of 5% in area 4 and increase of 6% in area 5; C3 case that presents the load level of C1 case and the disconnection of the transmission line 31–53. The scenarios were S1: All WADC-p, WADC-I, WADC-II, and WADC-III channels working and a time delay of 100 ms in all communication channels; S2: Time delay of 100 ms in all communication channels and the permanent communication loss of the speed signal of generator 14 (the third input of the WADC-p, WADC-I, WADC-II, and WADC-III); S3: All WADC-p, WADC-I, WADC-II, and WADC-III channels working and different time delays in the communication channels; S4: Different time delays in the communication channels and the permanent communication loss of the speed signal of generator 14 (the third input of the WADC-p, WADC-I, WADC-II, and WADC-III).

Considering T_i and T_o the time delays in the input and output of the WADC-p, WADC-I, WADC-II, and WADC-III, respectively, the different time delays used in scenarios S3 and S4 were $T1 = [T_i\ T_o] = [0.123\ 0.141]$. Fig. 3 presents the angular deviation responses of generators 15 and 16 for the C1, C2, and C3 operating conditions for the scenario S1 without WADC, with WADC-p, WADC-I, WADC-II, and WADC-III when a temporary three-phase fault-circuit of 50 ms was applied in the bus 40. Fig. 4 presents the angular deviation responses of generators 14 and 16 for the C1, C2, and C3 operating conditions for the scenario S2 without WADC, with WADC-p, WADC-I, WADC-II, and WADC-III and when a temporary three-phase fault-circuit of 50 ms was applied in the bus 40. Fig. 5 presents the angular deviation responses of generators 8 and 16 for the C1, C2, and C3 operating conditions for the scenario S3 without WADC, WADC-p, WADC-I, WADC-II,

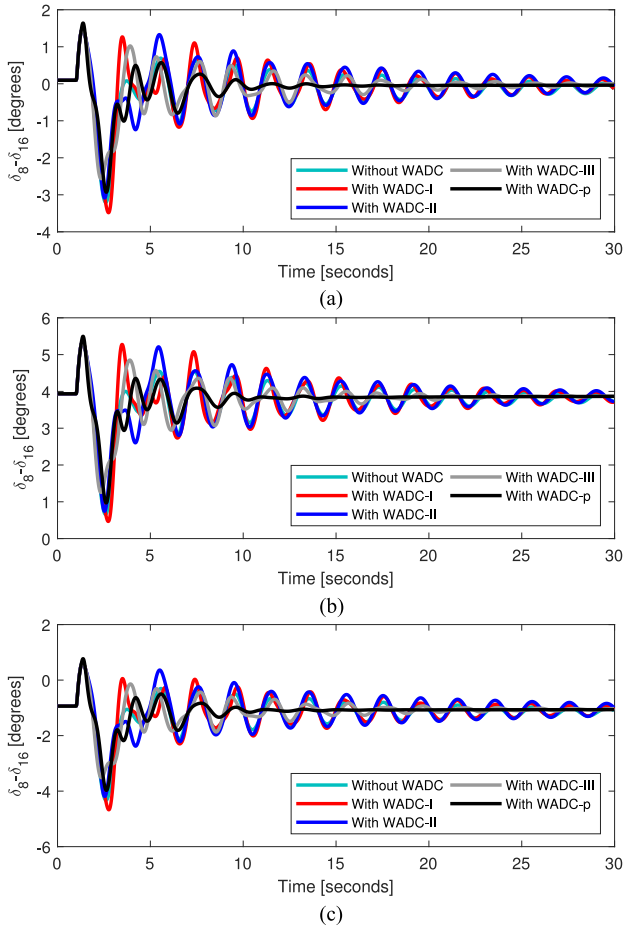

Fig. 5. Angular deviation responses of generators 8 and 16 without the WADC and with WADC-I, WADC-II, WADC-III, and WADC-p for the scenario S3 and (a) C1 operating condition, (b) C2 operating condition, and (c) C3 operating condition.

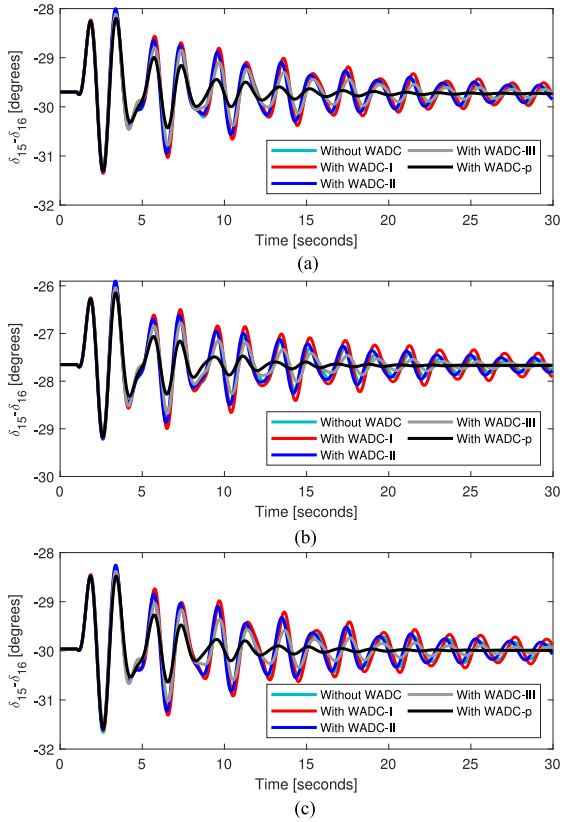

Fig. 6. Angular deviation responses of generators 15 and 16 without the WADC and with WADC-I, WADC-II, WADC-III, and WADC-p for the scenario S4 and (a) C1 operating condition, (b) C2 operating condition, and (c) C3 operating condition.

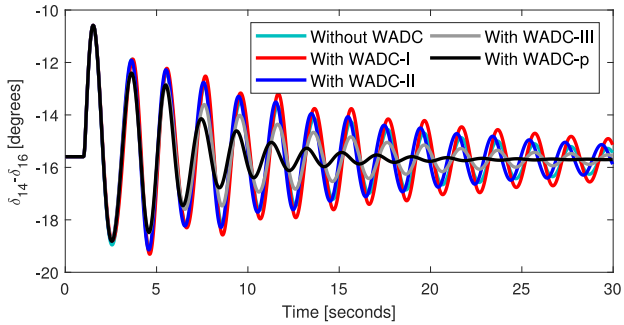

Fig. 7. Angular deviation responses of generators 14 and 16 without the WADC and with WADC-I, WADC-II, WADC-III, and WADC-p for a temporary 100 ms three-phase fault-circuit.

and WADC-III for the same temporary three-phase fault-circuit. Fig. 6 presents the angular deviation responses of generators 15 and 16 for the C1, C2 and C3 operating conditions for the scenario S4 without WADC, with WADC-p, WADC-I, WADC-II, and WADC-III for the same temporary three-phase fault-circuit.

The results for the power system with the proposed two-level controller, PSSs more the WADC-p, present a better damping performance than without the WADC (only the PSSs are working) and the designed controllers WADC-I, WADC-II, and WADC-III more the PSSs even when variations happen in the operating conditions and time delays of the WADC-p channels. Moreover, the angular responses for the system with the proposed two-level control structure present good performance even when one permanent communication failure of the WADC-p channel occurs. With the purpose of evaluating large disturbances, the C3 operation case was subjected to a 100 ms three-phase fault-circuit in the bus 40, the result is shown in Fig. 7 for the angular response of generator 14 in relation to 16, where again the angular response for the WADC-p controller performed better.

V. Conclusion

This article presented an algorithm based on LMIs to design a WADC to handling multiple operating conditions, time-delay uncertainties, and permanent communication failure of the WADC channels. Based on the algorithm development and achieved results, the power system with the two-level control structure can present a good power system dynamic performance, especially when interarea oscillation modes are presented. The quadratic stability provided by a polytopic model guarantees a good performance for a range of uncertainties in the operating conditions and time-varying delays. Besides, the

proposed LMI formulation includes the robustness to permanent communication failure of the WADC channels and the achieved results also proved the efficacy of the designed central controller for this kind of contingency.

REFERENCES

[1] F. Li *et al.*, "Smart transmission grid: Vision and framework," *IEEE Trans. Smart Grid*, vol. 1, no. 2, pp. 168–177, Sep. 2010.

[2] J. Zhao *et al.*, "Power system real-time monitoring by using PMU-based robust state estimation method," *IEEE Trans. Smart Grid*, vol. 7, no. 1, pp. 300–309, Jan. 2016.

[3] T. Prakash, S. R. Mohanty, and V. P. Singh, "PMU-assisted zone-3 protection scheme for PV integrated power systems immune to interharmonics," *IEEE Syst. J.*, vol. 14, no. 3, pp. 3267–3276, Sep. 2020.

[4] Y. Nie, Y. Zhang, Y. Zhao, B. Fang, and L. Zhang, "Wide-area optimal damping control for power systems based on the ITAE criterion," *Int. J. Electr. Power Energy Syst.*, vol. 106, pp. 192–200, Mar. 2019.

[5] B. P. Padhy, S. C. Srivastava, and N. K. Verma, "A Coherency-based approach for signal selection for wide area stabilizing control in power systems," *IEEE Syst. J.*, vol. 7, no. 4, pp. 807–816, Dec. 2013.

[6] T. Prakash, V. P. Singh, and S. R. Mohanty, "Cyber-attack resilient design of wide-area PSS considering practical communication constraints," *IEEE Syst. J.*, vol. 14, no. 2, pp. 2012–2022, Jun. 2020.

[7] L. Zacharia, M. Asprou, and E. Kyriakides, "Wide area control of governors and power system stabilizers with an adaptive tuning of coordination signals," *IEEE Open Access J. Power Energy*, vol. 7, pp. 70–81, 2020.

[8] M. E. C. Bento, D. Dotta, R. Kuiava, and R. A. Ramos, "Robust design of coordinated decentralized damping controllers for power systems," *Int. J. Adv. Manuf. Technol.*, vol. 99, no. 5/8, pp. 2035–2044, Nov. 2018.

[9] S. M. Azimi, R. A. Naghizadeh, and A. R. Kian, "Optimal controller design for interconnected power networks with predetermined degree of stability," *IEEE Syst. J.*, vol. 13, no. 3, pp. 3165–3175, Sep. 2019.

[10] M. E. C. Bento, D. Dotta, R. Kuiava, and R. A. Ramos, "Design of coordinated decentralized damping controllers for power systems considering uncertainties," *J. Control, Automat. Elect. Syst.*, vol. 29, no. 1, pp. 22–31, Feb. 2018.

[11] M. J. Morshed and A. Fekih, "A coordinated controller design for DFIG-based multi-machine power systems," *IEEE Syst. J.*, vol. 13, no. 3, pp. 3211–3222, Sep. 2019.

[12] M. E. C. Bento, "A hybrid procedure to design a wide-area damping controller robust to permanent failure of the communication channels and power system operation uncertainties," *Int. J. Elect. Power Energy Syst.*, vol. 110, pp. 118–135, Sep. 2019.

[13] Y. Zhou, J. Liu, Y. Li, C. Gan, H. Li, and Y. Liu, "A Gain scheduling wide-area damping controller for the efficient integration of photovoltaic plant," *IEEE Trans. Power Syst.*, vol. 34, no. 3, pp. 1703–1715, May 2019.

[14] M. E. C. Bento, R. Kuiava, and R. A. Ramos, "Design of wide-area damping controllers incorporating resiliency to permanent failure of remote communication links," *J. Control, Automat. Elect. Syst.*, vol. 29, no. 5, pp. 541–550, Oct. 2018.

[15] D. Dotta, A. S. e Silva, and I. C. Decker, "Wide-area measurements-based two-level control design considering signal transmission delay," *IEEE Trans. Power Syst.*, vol. 24, no. 1, pp. 208–216, Feb. 2009.

[16] M. E. C. Bento, D. Dotta, R. Kuiava, and R. A. Ramos, "A procedure to design fault-tolerant wide-area damping controllers," *IEEE Access*, vol. 6, pp. 23 383–23 405, 2018.

[17] M. Sarkar and B. Subudhi, "Fixed low-order synchronized and non-synchronized wide-area damping controllers for inter-area oscillation in power system," *Int. J. Electr. Power Energy Syst.*, vol. 113, pp. 582–596, Dec. 2019.

[18] M. Beiraghi and A. M. Ranjbar, "Additive model decision tree-based adaptive wide-area damping controller design," *IEEE Syst. J.*, vol. 12, no. 1, pp. 328–339, Mar. 2018.

[19] M. E. C. Bento, "A procedure to design wide-area damping controllers for power system oscillations considering promising input–output pairs," *Energy Systems*, vol. 10, no. 4, pp. 911–940, Nov. 2019.

[20] M. Bhadu, G. N. Sudha, N. Senroy, and I. Narayan Kar, "Robust linear quadratic gaussian-based discrete mode wide area power system damping controller," *IET Gener. Transmiss. Distrib.*, vol. 10, no. 6, pp. 1470–1478, Apr. 2016.

[21] B. Naduvathuparambil, M. Valenti, and A. Feliachi, "Communication delays in wide area measurement systems," in *Proc. 34th Southeast. Symp. Syst. Theory*. IEEE, 2002, pp. 118–122.

[22] W. Yao, L. Jiang, J. Wen, Q. Wu, and S. Cheng, "Wide-area damping controller for power system interarea oscillations: A networked predictive control approach," *IEEE Trans. Control Syst. Technol.*, vol. 23, no. 1, pp. 27–36, Jan. 2015.

[23] T. Prakash, V. P. Singh, and S. R. Mohanty, "A synchrophasor measurement based wide-area power system stabilizer design for inter-area oscillation damping considering variable time-delays," *Int. J. Electr. Power Energy Syst.*, vol. 105, pp. 131–141, Feb. 2019.

[24] Y. Shen, W. Yao, J. Wen, and H. He, "Adaptive wide-area power oscillation damper design for photovoltaic plant considering delay compensation," *IET Gener. Transm. Distrib.*, vol. 11, no. 18, pp. 4511–4519, Dec. 2017.

[25] W. Yao, L. Jiang, J. Wen, Q. H. Wu, and S. Cheng, "Wide-area damping controller of facts devices for inter-area oscillations considering communication time delays," *IEEE Trans. Power Syst.*, vol. 29, no. 1, pp. 318–329, Jan. 2014.

[26] C. Sharma and B. Tyagi, "Fuzzy Type-2 controller design for small-signal stability considering time latencies and uncertainties in PMU measurements," *IEEE Syst. J.*, vol. 11, no. 2, pp. 1149–1160, Jun. 2017.

[27] B. P. Padhy, S. C. Srivastava, and N. K. Verma, "Robust wide-area TS fuzzy output feedback controller for enhancement of stability in multimachine power system," *IEEE Syst. J.*, vol. 6, no. 3, pp. 426–435, Sep. 2012.

[28] L. Zacharia, M. Asprou, and E. Kyriakides, "Measurement errors and delays on wide-area control based on IEEE Std C37.118.1-2011: impact and compensation," *IEEE Syst. J.*, vol. 14, no. 1, pp. 422–432, Mar. 2020.

[29] C.-C. Sun, A. Hahn, and C.-C. Liu, "Cyber security of a power grid: State-of-the-art," *Int. J. Electr. Power Energy Syst.*, vol. 99, pp. 45–56, Jul. 2018.

[30] S. Liu, X. P. Liu, and A. El Saddik, "Denial-of-service (dos) attacks on load frequency control in smart grids," in *Proc. IEEE PES Innov. Smart Grid Technol. Conf.*, Feb. 2013, pp. 1–6.

[31] Y. Cao, X. Shi, Y. Li, Y. Tan, M. Shahidehpour, and S. Shi, "A simplified co-simulation model for investigating impacts of cyber-contingency on power system operations," *IEEE Trans. Smart Grid*, vol. 9, no. 5, pp. 4893–4905, Sep. 2018.

[32] S. Zhang and V. Vittal, "Design of wide-area power system damping controllers resilient to communication failures," *IEEE Trans. Power Syst.*, vol. 28, no. 4, pp. 4292–4300, Nov. 2013.

[33] S. Khosravani, I. Naziri Moghaddam, A. Afshar, and M. Karrari, "Wide-area measurement-based fault tolerant control of power system during sensor failure," *Electr. Power Syst. Res.*, vol. 137, pp. 66–75, Aug. 2016.

[34] S. Zhang and V. Vittal, "Wide-area control resiliency using redundant communication paths," *IEEE Trans. Power Syst.*, vol. 29, no. 5, pp. 2189–2199, Sep. 2014.

[35] M. E. Raoufat, K. Tomsovic, and S. M. Djouadi, "Dynamic control allocation for damping of inter-area oscillations," *IEEE Trans. Power Syst.*, vol. 32, no. 6, pp. 4894–4903, Nov. 2017.

[36] Y. Shen, W. Yao, J. Wen, H. He, and L. Jiang, "Resilient wide-area damping control using GrHDP to tolerate communication failures," *IEEE Trans. Smart Grid*, vol. 10, no. 3, pp. 2547–2557, May 2019.

[37] A. Yogarathinam and N. R. Chaudhuri, "A new MIMO ORC architecture for power oscillation damping using remote feedback signals under intermittent observations," *IEEE Syst. J.*, vol. 14, no. 1, pp. 939–949, Mar. 2020.

[38] C. Canizares, "Benchmark models for the analysis and control of small-signal oscillatory dynamics in power systems," *IEEE Trans. Power Syst.*, vol. 32, no. 1, pp. 715–722, Jan. 2017.

[39] P. Kundur, N. J. Balu, and M. G. Lauby, *Power System Stability and Control*. New York, NY, USA: McGraw-hill, vol. 7, 1994.

[40] M. Vajta, "Some remarks on Padé approximations," in *Proc. 3rd TEMPUS-INTCOM Symp. Intell. System. Control Meas.*, Sep. 2000, pp. 53–58.

[41] M. E. C. Bento, "Fixed low-order wide-area damping controller considering time delays and power system operation uncertainties," *IEEE Trans. Power Syst.*, vol. 35, no. 5, pp. 3918–3926, Sep. 2020.

[42] S. Gomes, N. Martins, and C. Portela, "Computing small-signal stability boundaries for large-scale power systems," *IEEE Trans. Power Syst.*, vol. 18, no. 2, pp. 747–752, May 2003.

[43] S. Boyd, L. El Ghaoui, E. Feron, and V. Balakrishnan, *Linear Matrix Inequalities in System and Control Theory*. Philadelphia, PA, USA: SIAM, Jan. 1994.

[44] J. F. Sturm, "Using SeDuMi 1.02, A Matlab toolbox for optimization over symmetric cones," *Optim. Methods Softw.*, vol. 11, no. 1/4, pp. 625–653, Jan. 1999.

[45] CEPEL, *Anatem User's Manual Version 10.5.2*. 2014, [Online]. Available: http://www.dre.cepel.br/